

Journal of Biomedical Optics

SPIEDigitalLibrary.org/jbo

Fiber-optic manipulation of urinary stone phantoms using holmium:YAG and thulium fiber lasers

Richard L. Blackmon
Jason R. Case
Susan R. Trammell
Pierce B. Irby
Nathaniel M. Fried

Fiber-optic manipulation of urinary stone phantoms using holmium:YAG and thulium fiber lasers

Richard L. Blackmon,^a Jason R. Case,^a Susan R. Trammell,^a Pierce B. Irby,^b and Nathaniel M. Fried^{a,c}

^aUniversity of North Carolina at Charlotte, Department of Physics and Optical Science, 9201 University City Avenue, Charlotte, North Carolina 28223-0001

^bCarolinas Medical Center, Department of Urology, 1023 Edgehill Road, Charlotte, North Carolina 28207

^cJohns Hopkins Medical Institutions, Department of Urology, 600 N. Wolfe Street, Baltimore, Maryland 21287

Abstract. Fiber-optic attraction of urinary stones during laser lithotripsy may be exploited to manipulate stone fragments inside the urinary tract without mechanical grasping tools, saving the urologist time and space in the ureteroscope working channel. We compare thulium fiber laser (TFL) high pulse rate/low pulse energy operation to conventional holmium:YAG low pulse rate/high pulse energy operation for fiber-optic suctioning of plaster-of-paris (PoP) stone phantoms. A TFL (wavelength of 1908 nm, pulse energy of 35 mJ, pulse duration of 500 μ s, and pulse rate of 10 to 350 Hz) and a holmium laser (wavelength of 2120 nm, pulse energy of 35 to 360 mJ, pulse duration of 300 μ s, and pulse rate of 20 Hz) were tested using 270- μ m-core optical fibers. A peak drag speed of \sim 2.5 mm/s was measured for both TFL (35 mJ and 150 to 250 Hz) and holmium laser (210 mJ and 20 Hz). Particle image velocimetry and thermal imaging were used to track water flow for all parameters. Fiber-optic suctioning of urinary stone phantoms is feasible. TFL operation at high pulse rates/low pulse energies is preferable to holmium operation at low pulse rates/high pulse energies for rapid and smooth stone pulling. With further development, this novel technique may be useful for manipulating stone fragments in the urinary tract. © The Authors. Published by SPIE under a Creative Commons Attribution 3.0 Unported License. Distribution or reproduction of this work in whole or in part requires full attribution of the original publication, including its DOI. [DOI: 10.1117/1.JBO.18.2.028001]

Keywords: holmium; lithotripsy; retropulsion; thulium; urinary stones.

Paper 12730 received Nov. 9, 2012; revised manuscript received Dec. 19, 2012; accepted for publication Dec. 21, 2012; published online Feb. 1, 2013.

1 Introduction

Our research group has previously studied the experimental thulium fiber laser (TFL) as a potential alternative to the clinical holmium:YAG laser for lithotripsy.¹⁻⁵ The superior TFL Gaussian beam profile has been focused to a diameter as small as 70 μ m, providing efficient coupling of higher laser energy into smaller fibers, thus leaving more irrigation space in the working channel, without hindering the flexibility of the ureteroscope.^{1,3} Furthermore, the TFL wavelength (1908 nm) more closely matches a major water absorption peak in tissue than does the holmium laser wavelength (2120 nm), leading to lower ablation thresholds and higher ablation rates.⁶ Finally, the TFL parameters (e.g., pulse length, pulse rate, and duty cycle) are more adjustable, thus providing more efficient stone ablation with reduced retropulsion and fiber tip degradation.²⁻⁴

During our previous TFL lithotripsy studies, we noticed that urinary stones were periodically attracted toward the fiber tip rather than pushed away from the fiber tip as would be expected from the cavitation-induced pressure wave. This phenomenon appeared more frequently as we conducted studies at higher TFL pulse rates. Previous investigators have reported movement of stones using the holmium laser that could be a result of this “suction effect,”⁷⁻⁹ but until now, this phenomenon has not been studied in detail. The TFL is capable of operating at low pulse energies and variable pulse rates and is therefore ideally suited

to reproduce this effect without risk of stone retropulsion, which has previously been demonstrated to be minimal using the TFL at pulse rates up to 150 Hz.⁴

Currently, stone stabilization devices utilizing numerous designs, including baskets, grasping tools, and “backstop” polymer material approaches, are being used to reduce stone retropulsion and increase ablation efficiency during holmium laser lithotripsy.¹⁰ However, these devices occupy valuable space inside the single working channel of the ureteroscope and add considerable expense to the surgical procedure. The objective of this study is to analyze the suction effect and determine its dependence on holmium laser pulse energy and TFL pulse rate. This study also explores the mechanism, presumably the pressure wave resulting from cavitation bubble collapse, that is responsible for the suction effect.

2 Methods

2.1 Laser Parameters

An experimental thulium fiber laser (TLR 110-1908, IPG Photonics, Oxford, Massachusetts) was operated at a wavelength of 1908 nm and externally modulated with a function generator (DS345, Stanford Research Systems, Sunnyvale, California) to produce a pulse duration of 500 μ s, similar to previous TFL lithotripsy studies.^{4,5} The TFL was operated at a constant pulse energy of 35 mJ while varying the pulse rate from 10 to 350 Hz. A clinical holmium:YAG laser (TwoPointOne XE, Coherent, Santa Clara, California) was operated at a wavelength of 2120 nm and fixed pulse duration of 300 μ s. The holmium

Address all correspondence to: Nathaniel Fried, University of North Carolina at Charlotte, Department of Physics and Optical Science, 9201 University City Avenue, Charlotte, North Carolina 28223-0001. Tel: +704-687-8149; Fax: 704-687-8197; E-mail: nmfried@uncc.edu.

laser was limited to operation at a relatively low pulse rate of 20 Hz while varying the pulse energy from 35 to 360 mJ.

2.2 Stone Suction Experiments

Spherical, 4-mm-diameter, plaster-of-paris stone phantoms with an average mass of 40.4 ± 2.0 mg were formed using a mold and sandpaper to smooth rough spots. These stones were used as an idealized stone model to eliminate potential variability due to stone shape and density. Previous investigators have also used PoP stone phantoms to model urinary stones because of their comparable tensile strength.^{11,12} Each stone was dried for at least 24 h and weighed using an analytical balance (AB54-S, Mettler-Toledo, Switzerland). The stones were monitored throughout the suction experiments, and any damaged stone was removed and replaced. A minimum of five PoP stone phantoms was used for each set of laser parameters in all of the studies.

Stones were placed in a saline bath on a level, flat surface with ruler markings. Laser energy was delivered through a 270- μ m-core optical fiber (Holmium Lightguide 270D, Olympus Gyrus ACMI, Southborough, Massachusetts) to the stone. The experiment was recorded with a camera at a frame rate of 30 Hz (73K3HN-YC, Mintron, Fremont, California). The fiber was positioned parallel to the surface of the saline bath, with energy being delivered slightly off-center, above the stone. The fiber was then pulled away from the stone at the maximum speed allowable to maintain stone movement without detachment. Figure 1 shows the experimental setup used to measure the stone velocity. Figure 2(a) and 2(b) shows representative images of the initial

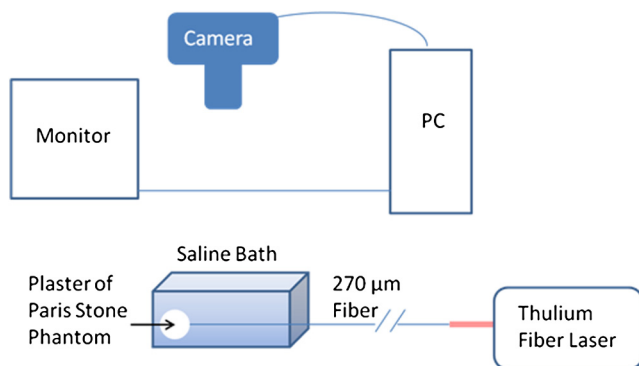


Fig. 1 Experimental setup used to record stone movement during laser fiber-optic manipulation.

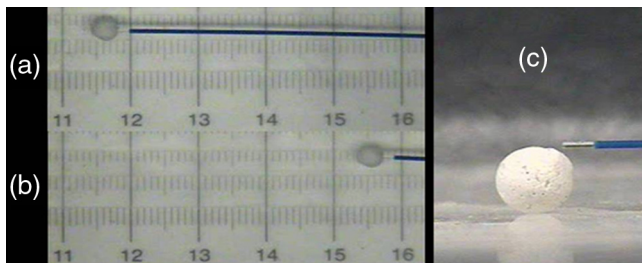


Fig. 2 Before (a) and after (b) snapshots of the 4-mm-diameter PoP stone being pulled by the 270- μ m-diameter fiber across a ruled surface in a saline bath using the holmium laser, operating at a pulse rate of 20 Hz and a pulse energy of 70 mJ. (c) Side view of fiber-to-stone orientation. Positioning of the fiber tip slightly off-center, above the stone, provided optimal stone manipulation.

and final stone locations after pulling for 16 s using the holmium laser at a pulse energy of 70 mJ. The velocity for each set of laser parameters was plotted using the recorded distance and time traveled by the stone. For the TFL, velocity versus pulse rate was plotted. For the holmium laser, velocity versus pulse energy was recorded. The fiber was placed slightly off-center and above the stone phantom for optimal manipulation [Fig. 2(c)].

2.3 Particle Image Velocimetry

Polymer microspheres (Duke Standards 4000 Series, Thermo Fisher Scientific, Waltham, Massachusetts) with diameters ranging from 30 to 50 μ m, refractive index of 1.59, and density of 1.05 g/cm³ were suspended in water. The microsphere density closely matched that of the water to ensure suspension in the water bath. The microspheres were illuminated from the side by a fiber-optic lamp. A 270- μ m-core fiber was inserted into the bath with the length of the fiber level with the surface. Laser energy was delivered in the water bath while videos of particle flow were recorded under magnification. The recorded particle flow was used to map the flow of water as a function of the laser parameters. This method examined the macroscopic effects of a train of laser pulses on the water flow.

2.4 Thermal Imaging

A thermal camera (SC655, FLIR, Billerica, Massachusetts) capable of a 50-Hz frame rate and 640 \times 480 resolution was used to track the flow of heated water as laser energy was delivered. The water bath was maintained near body temperature ($\sim 37^\circ\text{C}$). Similar to the particle image velocimetry (PIV) experiments described above, a 270- μ m-core fiber was inserted into the water bath with the length of the fiber level with the surface. Videos of the thermal signatures from heated water were recorded for TFL pulse rates of 10, 50, 100, 200, and 350 Hz. The thermal signature videos were compared to those using the microspheres as an alternative method to visualize the water flow caused by laser energy delivered in the water bath.

3 Results

3.1 Stone Suction Experiments

For the TFL, the effect of a net force pulling the stone toward the trunk end of the fiber was noticeable even at a low pulse energy and pulse rate of 35 mJ and 10 Hz, respectively [Fig. 3(a)]. The effect was weak, and no stone repulsion was observed. As the pulse rate was increased, the effect of the force pulling the stone toward the fiber tip became stronger. The stone pull velocity increased up to 250 Hz (although the increase between 75 and 250 Hz was not statistically significant). Each pulse caused the water to flow axially in two different directions. The water flow in both directions increased as the laser pulses were delivered at higher rates. The compounding effects of forces from each pulse acted on the stone by either pushing or pulling it away from the fiber tip, depending on where the fiber tip was placed with respect to the stone.

Furthermore, as the pulse rate was increased up to 250 Hz, strong repulsion forces were observed. This was a problem when trying to keep the stone attracted to the fiber tip. Because the effect of pulling or pushing the stone is dependent on where the fiber tip is placed, when the net repulsive force begins to dominate, the location of the fiber tip is critical. This may be the

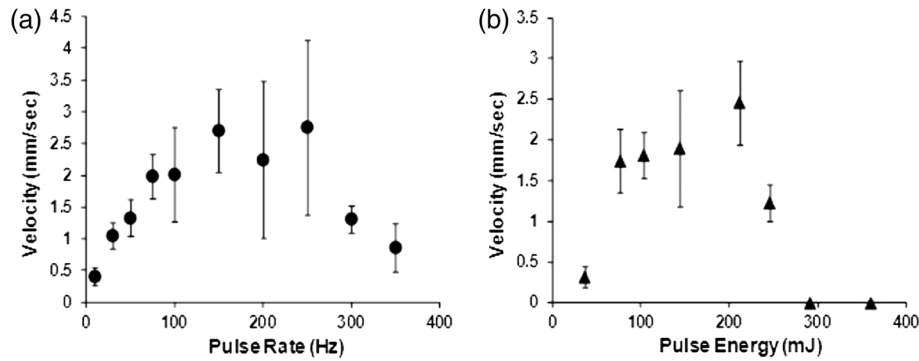


Fig. 3 (a) Stone pull velocity as a function of pulse rate for TFL pulse energy of 35 mJ. (b) Stone pull velocity as a function of pulse energy for a holmium laser pulse rate of 20 Hz.

cause for the high error bars in the midrange pulse rate data points shown in Fig. 3(a). Both repulsive and attractive forces were acting on the stone, and it was difficult to control which force dominated in the 200-Hz range.

As the pulse rate was increased to 350 Hz, repulsion forces dominated. The stone was not pulled as far without eventually being rapidly pushed away. One of the reasons for this effect is that the repulsion forces were so strong that a tightly wound vortex (to be seen in the PIV experiments) developed in close proximity to the fiber tip. Because the increase in water flow away from the fiber was stronger than the increase toward the fiber, the microspheres caught in the vortex were swept in the jet flowing away from the fiber tip.

The trend was similar for the holmium laser [Fig. 3(b)]. As the pulse energy was increased, the stone velocity also increased up to ~210 mJ (although the increase was not statistically significant for pulse energies between 70 and 210 mJ). The stone velocity then decreased as the pulse energy increased beyond 210 mJ. For operation at 35 mJ, the suction effect was observed without any repulsion effects. As the pulse energy was increased, the stone was pulled more rapidly, but in a discrete, choppy pattern of motion. The process of pulling the stone was not smooth, as experienced with the TFL. Use of higher pulse energies >70 mJ resulted in greater repulsion, which required the fiber to be held further away from the stone to maintain the suction effect. At pulse energies >210 mJ, the stone bounced randomly in all directions and repulsion was increasingly difficult to avoid. Pulse energies at 300 mJ and higher yielded a much different result than lower energies. The stone was either pushed far ahead of the fiber tip or pushed far behind the fiber tip in a quick, discrete motion. The attractive force at higher pulse energies required the fiber to be placed completely past the stone, with the potential clinical risk of the laser energy delivered by the fiber being absorbed by tissue structures directly in front of the fiber.

Figure 4 shows the stone pull velocity as a function of average power. This plot provides a direct comparison between holmium and TFL. The TFL was able to exploit the suction effect at more than double the power produced by the holmium laser. More power delivery could make it possible for the TFL to potentially exploit the suction effect to maximize stone ablation rates while minimizing stone repulsion.

3.2 Particle Image Velocimetry

Microspheres ranging from 30 to 50 μm in diameter were used to track the water flow during laser irradiation with both the TFL

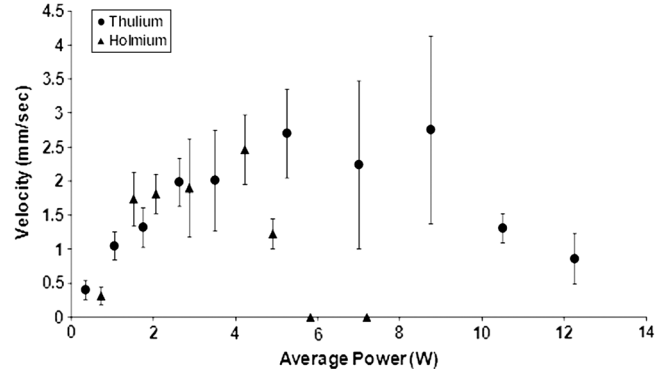


Fig. 4 Stone pull velocity for both lasers as a function of average power.

and holmium. The results of our study show two dominating but opposing forces during lithotripsy. One force, a repulsive force, is away from the fiber tip. The other force, an attractive force, is toward the fiber tip. The attractive force is suspected to be the cause of the suction effect observed during laser irradiation with both the thulium and holmium lasers.

Figure 5 illustrates the change in flow of the microspheres as the TFL pulse rate was increased. At low pulse rates, the microspheres flowed in two directions, toward and away from the fiber tip [Fig. 5(a)]. As pulse rates were increased, a vortex began to form around the sides of the fiber, causing microspheres pulled toward the fiber to return and become trapped in the jet flowing away from the fiber [Fig. 5(b)]. At pulse rates >250 Hz, the vortex surrounding the end of the fiber became tightly wound around the fiber tip [Fig. 5(c)]. This caused microspheres flowing toward the fiber tip to get trapped and then pushed back into the flow away from the fiber tip. This chaotic, tightly wound vortex is suspected to be the primary cause of decreasing stone pull velocity at higher pulse rates in the suction effect experiments.

The effects of the forces on the microspheres were more clear and consistent using the holmium laser than those of the TFL operating at 20 Hz with regard to the flow of microspheres. The vortices seen at higher pulse rates using the TFL were not seen using the holmium as pulse energies were increased. This could be due to the attractive force becoming stronger at roughly the same rate as the repulsive force. The experiments using the holmium showed that the speed at which the spheres moved away from the fiber tip, in both directions, increased as the pulse energy was increased.

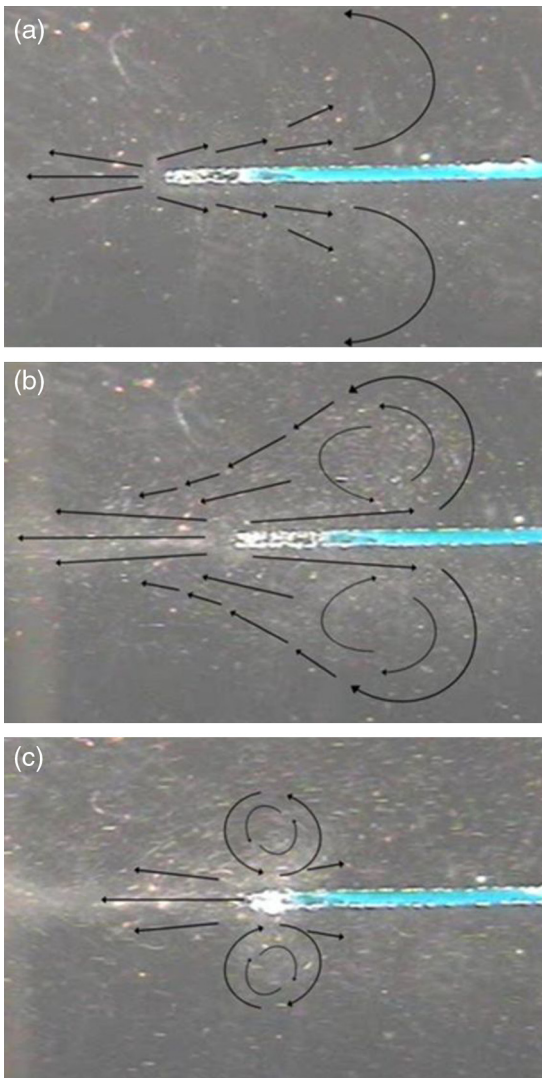


Fig. 5 Flow of microspheres for TFL pulse rates of 20 (a) 200 (b) and 350 (c) Hz at 35 mJ per pulse.

Although the frame rate of the camera used to capture the flow of microspheres was limited to 30 Hz, it was able to capture the shockwave-induced luminescence resulting from the collapse of the cavitation bubbles created by both TFL and holmium (Fig. 6). Such a distinct signature of cavitation bubbles has been previously reported as well.^{13,14} Figure 6 also shows distinct differences in the shape and formation of cavitation bubbles created using the TFL [Fig. 6(a)] and the holmium laser [Fig. 6(b)].

The modulated TFL operates at a longer pulse length (500 μ s) than the holmium (300 μ s). Furthermore, the absorption coefficient of water at the TFL wavelength ($\mu_a = 160 \text{ cm}^{-1}$) is five times greater than that of the holmium ($\mu_a = 28 \text{ cm}^{-1}$) (Ref. 1). Previous investigators have shown that for both increased absorption and longer pulse durations, the cavitation bubble becomes elongated and multiple cavitation bubbles may form.¹⁵⁻¹⁷ Indirect evidence of this is seen in both the results for the TFL microsphere experiments and the shockwave-induced luminescence observed emanating from two distinct points in front of the fiber tip [Fig. 6(a)].

The holmium-induced cavitation bubbles have been shown to be less elongated and pear shaped. This is also supported

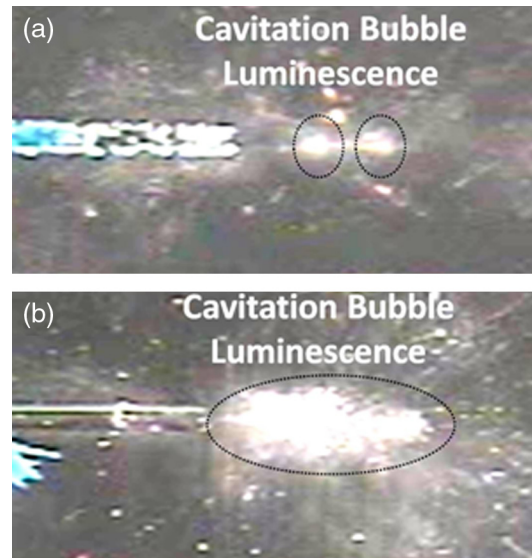


Fig. 6 Shockwave-induced luminescence resulting from the collapse of cavitation bubbles for TFL pulse rate of 350 Hz at 35 mJ pulse energy (a) and holmium pulse rate of 20 Hz at 35 mJ pulse energy (b).

by the results of the microsphere study performed with the holmium laser [Fig. 6(b)]. The area of luminescence appeared oval and resembled the shape of holmium-induced cavitation bubbles reported by other investigators.^{12,15,16,18,19}

3.3 Thermal Imaging

A thermal camera was used to track the flow of heated water as laser energy was delivered just beneath the surface of the water bath. For the TFL, the camera recorded a flow of heated water away from the fiber tip and toward the trunk end of the fiber. The thermal camera also recorded small thermal eddies near the fiber tip. Figure 7 shows a recorded video frame. As the TFL pulse rate was increased, the area of thermal flow also increased. Thermal images (not shown here) were also acquired while heating water using the holmium laser, but no discernible eddies or flow pattern were observed. This may be due to the longer optical penetration depth of the holmium laser wavelength in water, resulting in a wider spread of water heating. The videos captured

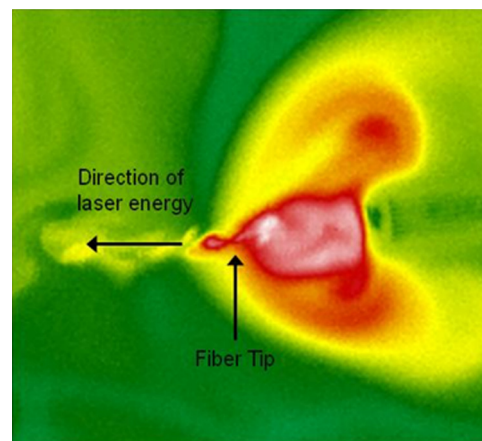


Fig. 7 Frame of a thermal video captured during fiber-optic delivery of the TFL energy at 35 mJ and 200 Hz in a water bath.

with the thermal camera reinforced the validity of trends observed in the suction effect and particle velocimetry studies.

4 Discussion

Our laboratory has studied the thulium fiber laser as a potential alternative to the holmium laser in lithotripsy. The TFL Gaussian spatial beam profile is better suited for coupling into smaller optical fibers. Use of smaller fibers in turn allows more flexible ureteroscope deflection and increased irrigation rates during lithotripsy. Furthermore, the TFL wavelength closely matches a major water absorption peak. Because a major absorber of laser energy in kidney stones is water, the higher absorption coefficient translates to more efficient urinary stone ablation. Finally, the TFL is capable of operating at variable pulse durations and rates. We have previously demonstrated that increased TFL pulse rates and complex modulation of pulse trains can lead to more efficient stone ablation while limiting negative effects such as retropulsion or fiber tip degradation. This flexible TFL operation with variable parameters makes it a suitable candidate for exploitation of the suction effect as well.

Previous investigators have reported the role of cavitation bubble dynamics during holmium laser lithotripsy.^{8,12,16,20–22} Some of these reports have shown images of small residual effects of the bubble collapse behind the fiber tip.^{12,19} This is presumably due to a collapsing bubble-induced pressure wave propagating in the axial direction of the fiber, both toward and away from the fiber tip. Although this pressure wave has been observed to be too weak to induce photomechanical ablation of urinary stones, it has been shown to be sufficiently strong to push stones away from the fiber tip. This study investigated in further detail the pressure wave reported in previous studies that may be responsible for the suction effect.^{19,20,23–25} A recent study has also reported that during the collapse of micrometer-sized bubbles the maximum pressure of the shock wave emitted during bubble rebound can be an order of magnitude smaller than that induced by millimeter-sized bubbles.²⁶ Future studies utilizing a high-speed camera for direct imaging of cavitation bubble dimensions and dynamics during both Ho:YAG and TFL lithotripsy may address how large the bubble must be for the suction effect to be observed.

There are many potential clinical applications for the suction effect. The most direct use would be to manipulate urinary stones in the kidney or bladder. Because the TFL is able to produce the suction effect at pulse rates that do not result in retropulsion, a stone could be trapped at the fiber tip and then transported to a more desirable location for stone ablation. If the stone is sufficiently small, the suction effect could also potentially be used to navigate the stone out of the urinary tract. Furthermore, when using the TFL, the suction effect is dominant over retropulsion at pulse rates ideal for stone ablation (up to 150 Hz).⁴ This may provide the possibility of trapping the stone at the fiber tip during stone ablation. Ideally, the stone would bounce around the fiber tip while it is broken down. Overall, exploitation of the suction effect would theoretically provide an urologist with greater control during laser lithotripsy without the need for stone stabilization devices.

Although the reproduction and quantification of the suction effect is possible, it requires further study. Our results show high error bars, mainly due to human error in positioning the fiber tip in the most efficient location relative to the stone to utilize the suction effect. A urologist may have even less control

positioning the fiber around the stone. This limitation must be overcome before the suction effect can be viable for surgical application. Also, the suction effect is dependent on stone size. The effect is not as strong as stone size increases. The shape of the stone may also play a role in the strength of the suction effect. Finally, our studies were performed in a stable environment. The drag force of motionless saline was the only major force acting against the stone. Other forces, such as saline flow through the working channel of the ureteroscope, may also play a significant role in whether the stone can be trapped by the attractive forces responsible for this suction effect.

Our knowledge of the suction effect is not yet sufficient for use in practical applications. Further studies need to be conducted to overcome these current limitations. Pulse duration, pulse energy, pulse distribution, stone size, stone shape, and environment all need to be further explored in more detail. Computer simulations may also be necessary to assist in the optimization of this large matrix of parameters.

5 Conclusions

This study has demonstrated the ability of both the holmium:YAG and thulium fiber lasers to rapidly and reproducibly pull stone phantoms with proper placement of the optical fiber and optimal choice of laser parameters. Future studies may focus on the role of this “suction effect” as a tool to manipulate urinary stones during laser lithotripsy. This phenomenon may also ideally be used to limit the movement of stone fragments during ablation, thus potentially eliminating the need for a stone stabilization device.

Acknowledgments

This research was supported, in part, by a Collaborative Research Grant between UNC-Charlotte and the Carolinas Medical Center and a Faculty Research Grant from UNC-Charlotte. Richard Blackmon is supported by a National Science Foundation Graduate Fellowship.

References

1. N. J. Scott, C. M. Cilip, and N. M. Fried, “Thulium fiber laser ablation of urinary stones through small-core optical fibers,” *IEEE J. Sel. Top. Quantum Electron.* **15**(2), 435–440 (2009).
2. R. L. Blackmon, P. B. Irby, and N. M. Fried, “Holmium:YAG ($\lambda = 2, 120$ nm) versus thulium fiber ($\lambda = 1, 908$ nm) laser lithotripsy,” *Lasers Surg. Med.* **42**(3), 232–236 (2010).
3. R. L. Blackmon, P. B. Irby, and N. M. Fried, “Thulium fiber laser lithotripsy using tapered fibers,” *Lasers Surg. Med.* **42**(1), 45–50 (2010).
4. R. L. Blackmon, P. B. Irby, and N. M. Fried, “Comparison of holmium:YAG and thulium fiber laser lithotripsy: ablation thresholds, ablation rates, and retropulsion effects,” *J. Biomed. Opt.* **16**(7), 071403 (2011).
5. R. L. Blackmon, P. B. Irby, and N. M. Fried, “Enhanced thulium fiber laser lithotripsy using micro-pulse train modulation,” *J. Biomed. Opt.* **17**(2), 028002 (2012).
6. E. D. Jansen et al., “Temperature-dependence of the absorption-coefficient of water for midinfrared laser-radiation,” *Lasers Surg. Med.* **14**(3), 258–268 (1994).
7. P. Kalra, N. B. Le, and D. Bagley, “Effect of pulse width on object movement in vitro using holmium:YAG laser,” *J. Endourol.* **21**(2), 228–231 (2007).
8. H. Lee et al., “Stone retropulsion during holmium:YAG lithotripsy,” *J. Urol.* **169**(3), 881–885 (2003).
9. T. D. White et al., “Evaluation of retropulsion caused by holmium:YAG laser with various power settings and fibers,” *J. Endourol.* **12**(2), 183–186 (1998).

10. C. J. Pagnani, M. El Akkad, and D. H. Bagley, "Prevention of stone migration with the accordion during endoscopic ureteral lithotripsy," *J. Endourol.* **26**(5), 484–488 (2012).
11. C. G. Marguet et al., "In vitro comparison of stone retropulsion and fragmentation of the frequency doubled, double pulse Nd:YAG laser and the holmium:YAG laser," *J. Urol.* **173**(5), 1797–1800 (2005).
12. H. W. Kang et al., "Dependence of calculus retropulsion on pulse duration during holmium:YAG laser lithotripsy," *Lasers Surg. Med.* **38**(8), 762–772 (2006).
13. C. D. Ohl et al., "Bubble dynamics, shock waves and sonoluminescence," *Phil. Trans. R. Soc. London A* **357**(1751), 269–294 (1999).
14. A. A. Buzukov and V. S. Teslenko, "Sonoluminescence following focusing of laser radiation into liquid," *JETP Lett.* **14**(5), 189–191 (1971).
15. M. Frenz et al., "Comparison of the effects of absorption coefficient and pulse duration of 2.12- μm and 2.79- μm radiation on laser ablation of tissue," *IEEE J. Quantum Electron.* **32**(12), 2025–2036 (1996).
16. P. Zhong et al., "Transient cavitation and acoustic emission produced by different laser lithotripters," *J. Endourol.* **12**(4), 371–378 (1998).
17. K. F. Chan et al., "Erbium:YAG laser lithotripsy mechanism," *J. Urol.* **168**(2), 436–441 (2002).
18. T. Lu et al., "Cavitation effect of holmium laser pulse applied to ablation of hard tissue underwater," *J. Biomed. Opt.* **15**(4), 048002 (2010).
19. T. Asshauer, K. Rink, and G. Delacretaz, "Acoustic transient generation by holmium-laser-induced cavitation bubbles," *J. Appl. Phys.* **76**(9), 5007–5013 (1994).
20. K. F. Chan et al., "Holmium:YAG laser lithotripsy: a dominant photo-thermal ablative mechanism with chemical decomposition of urinary calculi," *Lasers Surg. Med.* **25**(1), 22–37 (1999).
21. S. S. Spore et al., "Holmium:YAG lithotripsy: optimal power settings," *J. Endourol.* **13**(8), 559–566 (1999).
22. A. Vogel, "Nonlinear absorption: intraocular microsurgery and laser lithotripsy," *Phys. Med. Biol.* **42**(5), 895–912 (1997).
23. B. Han et al., "Mechanical effects of laser-induced cavitation bubble on different geometrical confinements for laser propulsion in water," *Opt. Lasers Eng.* **49**(3), 428–433 (2011).
24. E. A. Brujan et al., "The final stage of the collapse of a cavitation bubble close to a rigid boundary," *Phys. Fluids* **14**(1), 85–92 (2002).
25. A. Vogel and W. Lauterborn, "Acoustic transient generation by laser-produced cavitation bubbles near solid boundaries," *J. Acoust. Soc. Am.* **84**(2), 719–731 (1988).
26. A. Brujan and Y. Matsumoto, "Collapse of micrometer-sized cavitation bubbles near a rigid boundary," *Microfluid. Nanofluid.* **13**(6), 957–966 (2012).